RSC Advances

ROYAL SOCIETY OF CHEMISTRY

www.rsc.org/advances

Cite this: DOI: 10.1039/c0xx00000x

www.rsc.org/xxxxxx

ARTICLE TYPE

Controllable synthesis of silver nanoparticles in hyperbranched macromolecule templates for printed flexible electronics

Zhiliang Zhang,*[ab] and Huayong Zhang[a]

Received (in XXX, XXX) Xth XXXXXXXXX 20XX, Accepted Xth XXXXXXXXX 20XX

DOI: 10.1039/b000000x

In this work, a series of different generation hyperbranched macromolecules were synthesized and exploited to template-directed synthesis of silver nanoparticles (AgNPs). The results of UV-vis spectra, transmission electron microscopy and scanning electron microscopy images showed that the synthesized AgNPs was nearly uniform, monodisperse and the mean AgNPs size were 31.2±3.6, 25.6±2.7 and 21.8±2.2 nm corresponding to the respective generation hyperbranched macromolecules. Based on the as-synthesized AgNPs, a sequence of flexible electrocircuits were successfully fabricated by ink-jet printing technique and exhibited very low resistivity in the range of 8.26×10^{-8}~7.62×10^{-8} Ω.m after laser sintering treatment. This method provided a facile and efficient strategy to synthesize uniform and monodisperse AgNPs, and would have enormous potential in the application for flexible electronics, electrochemical devices and biosensors assembly.

Introduction

Flexible electronics has received considerable attentions in recent years as it exhibits tremendous application potentiality in optoelectronics such as solar cells,[1] LCDs,[2] OLED lighting,[3, 4] touch screen panels devices. [5-7] As a rapid direct-writing pattern approach, ink-jet printing technique is recognized as the most convenient and effective method to fabricate various conductive patterns on the flexible substrates.[8] Compared with the other fabrication methods, this approach offers an ideal alternative to conventional photolithography as it can deliver the precise quantities of conductive materials to desired locations to fabricate various electronic devices. In addition, ink-jet printing technique is an environment-friendly approach for mass-production of electrocircuits since it can avoid producing large quantities of chemical waste and eliminate conventionally complex photolithography process.[9, 10]

At present, the major obstacle in utilizing ink-jet printing technique to fabricate flexible electrocircuits, is to explore a facile and low-cost strategy to synthesize uniform and monodisperse metal nanoparticles, which is extremely pivotal to attain the fluent printing process and high electrical conductivity at low sintering temperature. To date, a wide variety of methods, such as microemulsion,[11] solvothermal reduction,[12] microwave irradiation,[13] sonochemical reduction[14] and chemical reduction,[15] have been employed to synthesize metal nanoparticles. Among these methods, chemical reduction was the most preferred due to its simplicity, low-cost and proportional massive scaling-up.[16] However, it is difficult to obtain uniform and monodisperse nanoparticles with chemical reduction method in common condition. As a result, the ink stability based on these synthesized nanoparticles would be likely affected as they aggregate and precipitate out from the solution. More seriously, the printer nozzle would be clogged with these larger nanoparticles or aggregation.[17] Although intensive efforts have been devoted to this stubborn problem, it still remains a big challenge to develop a facile and effective approach to synthesize uniform and monodisperse nanoparticles in order to effectively eliminate aggregation and clogs.

It is well known that the size distribution and agglomeration extent of metal nanoparticles could be effectively controlled by regulating the protected templates.[18] The strategy to achieve this goal is to control the growth of nanoparticles in monodisperse templates, such as porous membranes, dendrimers or reversed micelles.[19-21] As a special monodisperse macromolecule with successive layers or generations of branch units surrounding a central core, dendrimer is considered as a superb template to synthesize metal nanoparticles with narrow size distribution owing to their unique molecule properties.[22-24] The synthesized nanoparticles with dendrimer template exhibit obvious improvement on monodispersity and aggregation. However, the synthesis of dendrimers requires cost-intensive and time-consuming multistep procedure, and it severely restricts dendrimers as template to synthesize monodisperse nanoparticles and the further application of ink-jet printing technique in flexible electronics fields.

In contrast to dendrimers, hyperbranched macromolecules (HBMs) can be obtained by a single-step synthesis or commercially available in quantities.[25] More importantly, HBMs exhibit quite similar molecule structure and properties with dendrimers. Firstly, HBMs possess an intrinsically well-defined globular structure and dendritic-branched molecule structure, which can serve as gates to control the access of metal iron into the macromolecules interior cavities, and consequently

effectively improve the monodispersity by regulate the nucleation and growth of crystal nucleus. Secondly, HBMs have highly functional terminal groups on the molecule periphery, and these terminal groups are super capping agents to be anchored on the surfaces of nanoparticles, which can effectively prevent the agglomeration from the ink. Therefore, HBMs is another excellent template candidate for generating monodisperse nanoparticles without agglomeration.[26, 27]

Although some study is concerned on the synthesis of metal nanoparticles with dendrimers or HBMs, the application of AgNPs with HBMs as templates for inkjet printed flexible electronics is up to now still not reported. Following our previous study on AgNPs and HBMs,[28-30] we here developed a facile and efficient strategy to synthesize AgNPs with HBMs as template for flexible electronics. In this work, a series of HBMs with pentaerythritolas as core were synthesized and used to template-directed synthesis of AgNPs. The results showed that the synthesized AgNPs was nearly uniform and monodisperse, and the mean nanoparticles diameter were 31.2±3.6, 25.6±2.7 and 21.8±2.2 nm corresponding to the respective generation HBMs. More importantly, the conductive ink fabricated by our strategy exhibited high stability due to the highly density functional terminal groups anchored on the surfaces of AgNPs. A series of electrocircuits were fabricated by ink-jet printing the as-synthesized AgNPs on polyethylene terephthalate (PET) substrate. After the laser sintering treatment, the printed electrocircuits exhibited very low resistivity in the range of 8.26×10^{-8}~7.62×10^{-8} Ω.m. By employing HBMs to template-directed synthesis of AgNPs, we achieved both full control size distribution and effectively prevented AgNPs aggregation. This strategy successfully provided a facile and efficient method to synthesize nearly uniform and monodisperse AgNPs, and would have enormous potential for flexible electronics.

Experimental

Chemicals

Silver nitrate, D-glucose and p-toluene sulphonic acid were obtained from Alfa Aesar CO., LTD. Methyl methacrylate, 2,2'-Dihydroxydiethylamine, pentaerythritol, polyethylene glycol (PEG) and sodium citrate were purchased from American Sigma CO., LTD. Ethanol, acetone and ethylene glycol were obtained from Beijing Chemical Co. The other chemicals were analytical or high-reagent grade, and all these chemicals and materials were used as received without further purification. The water used throughout the experiments was ultrapure water (18.2 MΩ) produced by a Milli-Q system.

Synthesis of HBMs based on pentaerythritol as core

The N,N-diethylol-3-amine methylpropionate was synthesized according to the literature.[28] Methyl acrylate (0.5 mol), diethanolamine (0.5 mol) and methanol (50 mL) were added into a 100 mL three-necked flask, the admixture was stirred at 35 ◦C for 4 h, then removed the methanol by vacuumizing and N,N-diethylol-3-amine methylpropionate was obtained.

A series of HBMs with hydroxyl as terminal group was synthesized following a typical process (Fig. S1). Pentaerythritol (0.1 mmol), N,N-diethylol-3-amine methylpropionate (6.0 mmol) and p-toluene sulphonic acid (0.028 mmol) were added into a three-necked flask. The mixture were heated to 120 °C and kept for 2 h. After purification, the final product was the fourth generation (G4) HBMs with pentaerythritol as core, where Gn referred to the generation number. Changing the molar ration of pentaerythritol and N,N-diethylol-3-amine methylpropionate, with the similar synthesis procedure, the fifth and sixth generation (G5 and G6) of HBMs were received respectively.

HBMs template-directed synthesis of AgNPs

AgNPs synthesized with G4 HBMs as template were executed by a very straightforward, one-phase reaction. In a typical synthesis process, 20 mL aqueous solution containing 60 mg silver nitrate was slowly added into a beaker containing 120 mg G4 HBMs in 20 mL aqueous solution, and stirred for 15 min to form Ag-HBMs complex. Next, the complex was reduced by slow addition of freshly prepared aqueous solution of D-glucose. The products were purified by washing with water, and separated with centrifugation. After drying under vacuum at 60℃ for 30 min, bright-yellow powders were obtained. AgNPs synthesized with G5 or G6 HBMs as templates were received respectively with the similar procedure.

Fabrication of flexible electrocircuits by ink-jet printing technique

The synthesized AgNPs were redissolved into the mixture of ethylene glycol, ethanol and water with a mass ratio of about 7:2:1, and dispersed by ball milling to obtain 12 wt% AgNPs ink for fabricating the ink-jet printed flexible electrocircuits. According the designs, a series of electrocircuits were fabricated by ink-jet printing the AgNPs ink onto PET substrates using Dimatix Fujifilm DMP-2831 printer with 10 pL Dimatix materials cartridge controlled by the Dimatix Drop Manager software. The printing frequency was set at 5.0 kHz and a customized waveform was used, which had a maximum voltage of 22 V and a pulse width of 8.5 μs. The substrate temperature was set to 30 °C, and the humidity within the printing chamber was 30-40% RH. The printed electrocircuits were sintered by a semiconductor laser (808 nm, 0.8 W) to improve the conductivity. The laser beam onto a spot remained with approximately 2 mm in diameter and moved with 0.2 mm/s velocity along the direction of printed electrocircuits at room temperature.

Characterization

The UV-vis and X-ray diffraction (XRD) spectra of AgNPs were collected using a Hitachi U-4100 spectrophotometer and Bruker D8 X-ray diffractometer respectively. The transmission electron microscopy (TEM) images were obtained with JEM-1010 transmission electron microscope at 60 kV. The samples were prepared by placing two or three drops of the dilute AgNPs dispersion in alcohol on carbon-coated copper grids. X-ray photoelectron spectroscopy (XPS) was recorded on ESCALab 220i-XL electron spectrometer from VG Scientific using 300 W Al Kα radiation, and the base pressure was about 3×10^{-9} mbar. The scanning electron microscopy (SEM) images were investigated by Hitachi S-4800 scanning electron microscopy. Size distribution and number-average particle diameters were obtained using the Image ProPlus Image Analysis System. The optical images of printed electrocircuits were obtained by Olympus MX40 optical microscope. The cross-sectional area of

Cite this: DOI: 10.1039/c0xx00000x

www.rsc.org/xxxxxx

ARTICLE TYPE

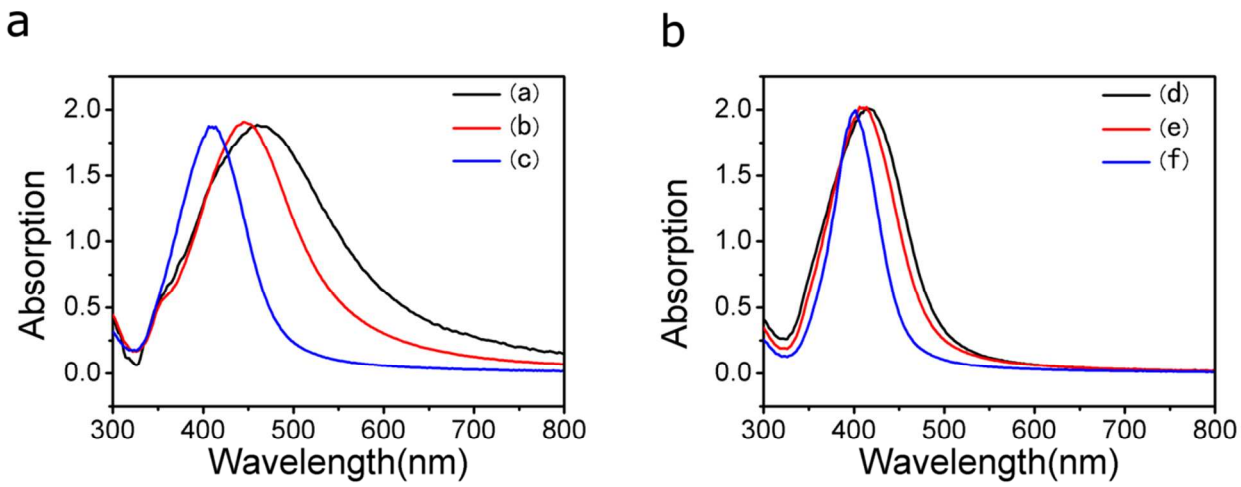

Fig. 1 (a) UV-vis spectra of the synthesized AgNPs with the protected templates sodium citrate (460 nm, curve **a**), PEG (442 nm, curve b) and G5 HBMs (412 nm, curve c) respectively; (b) UV-vis spectra of the synthesized AgNPs with the protected templates G4 HBMs (416 nm, curve d), G5 HBMs (412 nm, curve e) and G6 HBMs (406 nm, curve f) respectively.

the printed electrocircuits was determined in the Kosaka ET4000 surface profiler. The resistance of the fabricated pattern was measured on a Keithley 4200-SCS semiconductor analyzer with two point test method at 25 ℃. The electrical resistivity, ρ, was calculated from the resistance R, the length l, and the cross-sectional area A of the line, using $\rho = RA/l$.

Results and discussion

The shape and size distribution of the AgNPs were fairly pivotal for the printed flexible electronics to attain a fluent printing process. In order to achieve homogeneous particle size and shape, the choice of templates was extremely important. Fig. 1(a) showed UV-vis spectra of the synthesized AgNPs as the templates were sodium citrate (460 nm, curve a), PEG (442 nm, curve b) and G5 HBMs (412 nm, curve c) respectively. According to Mie's theory,[31] the position and shape of plasma absorption was strongly dependant on the nature of the metal nanoparticles, such as the size, shape, and status of aggregation. From Fig. 1(a), the absorption shapes in curve (a)-(c) were almost symmetrical, and this revealed that the synthesized AgNPs protected by these templates were not agminated. Moreover, the absorption peak in curve (a)-(b) shifted toward red wavelength and exhibited more broad half-peak breadth compared with that in curve (c), which indicated that the synthesized AgNPs protected by PEG and sodium citrate possessed larger size and more wide distribution than those by G5 HBMs.[32, 33] These preliminary results suggest that HBMs could be used to template--directed synthesis of nearly uniform and monodisperse AgNPs.

In order to investigate the structure influence on the size and distribution, the HBMs with generations from G4 to G6 were exploited to template-directed synthesis of AgNPs. From Fig. 1(b), the absorption position for curves (d)-(f) was determined to be at 416, 412, and 406 nm, corresponding to G4, G5, and G6 HBMs generation, respectively. The absorption peaks showed a little blue shift and exhibited narrower half-peak breadth with the HBMs generation increase, which indicated that the formed AgNPs had smaller size and narrower distribution. In addtion, the curves in Fig. 1(b) were very symmetrical, and this stated that HBMs could be readily anchored on the AgNPs surface and effectively prevented the agglomeration. All these results were further confirmed by TEM analysis in Fig. 2(a)–(f).

In theory, the nanoparticle size and distribution from a chemical synthesis process was closely related to the protected templates due to the nucleation, growth and agglomeration.[34] In Fig.2(a)-(c), TEM images of AgNPs with sodium citrate, PEG and G5 HBMs were presented respectively. Compared the images in Fig. 2, the AgNPs in Fig. 2(a)-(b) were irregular, bigger, and had more broad size distribuion, which was in good agreement with the trend of plasmon absorption band (Fig. 1a, curve (a) and curve (b)). It was probably because that overfull crystal nucleus were formed for an instant when the reductants were added into the reaction system. As protected templates, citrate and PEG could not promptly absorb onto the surface of nucleus at this moment, accordingly, resulting the nucleus aggregation into irregular and bigger nanoparticles. In contrast, as an excellent template for generating nanoparticles, HBMs possessed sufficient interior cavity and terminal groups in macromolecules, which could effectively regulate the nucleation and growth process and prevent the agglomeration. As a result, the obtained AgNPs in Fig. 2(c) exhibted nearly uniform morphology and monodisperse distribution.

Furthermore, the influence of HBMs generation on the size and distribution were further investigated. From Fig.2(d)-(f), all

Cite this: DOI: 10.1039/c0xx00000x

www.rsc.org/xxxxxx

ARTICLE TYPE

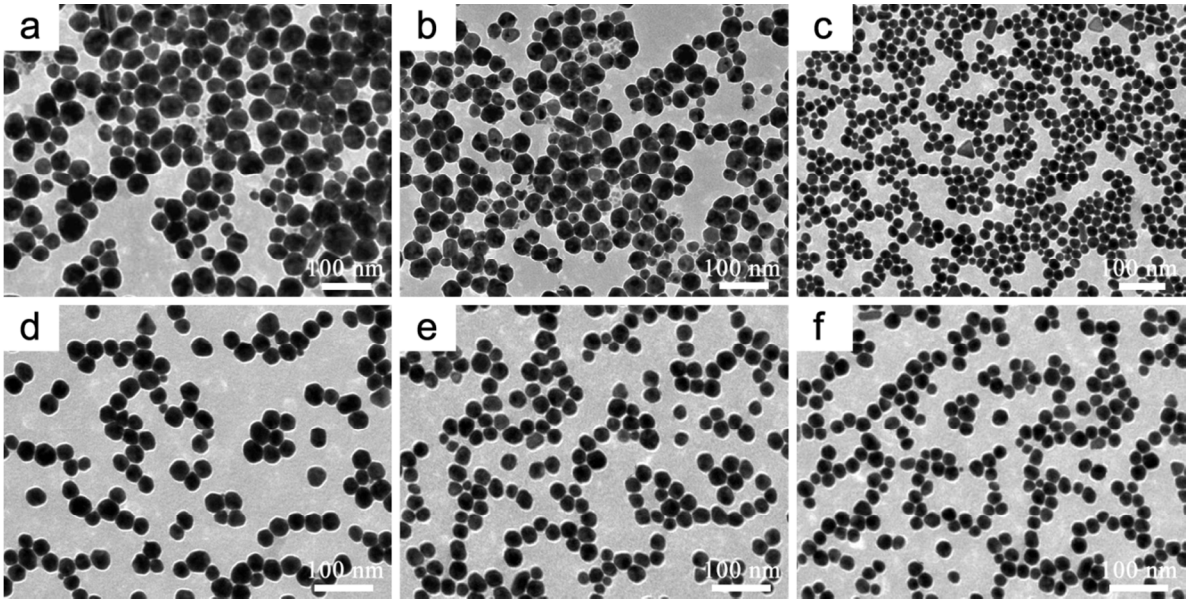

Fig. 2 TEM images of the AgNPs encapsulated with sodium citrate (a), PEG (b) and G5 HBMs (c); TEM images of the AgNPs encapsulated with G4 (d), G5 (e) and G6 HBMs (f) respectively.

AgNPs were almost spherical and had a narrow size distribution. A careful comparison of size distribution histograms in Fig. S2, it was clearly demonstrated that the mean size of the synthesized AgNPs decreased from 31.2±3.6 to 21.8±2.2 nm with the generation of HBMs increase from G4 to G6, which was also supported by the plasmon absorption band (Fig.1b, curve (d)-curve (f)). It was noteworthy that the size distribution of the synthesized AgNPs became narrower with the increase of HBMs generation, which suggested that the structure of HBMs played an important role and could efficiently prevent aggregation as protected templates during the AgNPs synthesis procedure.

An understanding of the size and distribution change with HBMs generation could now be obtained by examining the process involved in the build-up to the AgNPs. It has been postulated that silver ions could coordinate with the terminal groups to form Ag-HBMs complex at the surface and interior of the macromolecules, then the AgNPs formation would generally take place in the internal cavity of HBMs molecules or among the HBMs molecules. When G4 HBMs were used, the internal cavities were bigger and the steric effect was smaller, so its capability to prevent AgNPs from aggregation was relatively weaker. As the structure evolved to G5 HBMs, the internal environment started to get defined, and more so in G6 HBMs, creating smaller cavities around the central pentaerythritol core. Moreover, the stereo-hindrance effect of G5 and G6 HBMs was higher compared with G4 HBMs, and their capability to prevent AgNPs from aggregation was highly enhanced. Consequently, the mean size and distribution became smaller with HBMs generation increase. From the above results, nearly uniform and monodisperse AgNPs with the size about 20-30 nm could be achieved by this facile method, which proved that the HBMs could be an ideal template to synthesize ideal AgNPs for ink-jet printed flexible electronics.

To gain more information on the encapsulation state of the AgNPs, XPS technique was employed to detect the composition of the purified AgNPs, and the binding energy was referenced to the standard C1s at 287.60 eV. Fig 3(a) showed the XPS survey spectra of the AgNPs sample. In the spectra, the atoms of C, N, O and Ag were all clearly detected, and no obvious other peaks were found, indicating the high purity of the sample. Fig. 3 also presented high-resolution XPS spectra displaying the (b) Ag 3d, (c) C 1s, and (d) O 1s spectral regions. From the spectra of Ag3d (Fig.3b), the binding energies for $Ag3d_{5/2}$ and $Ag3d_{3/2}$ were identified at 367.85 eV and 373.62 eV respectively. In fact, these values were compared to the respective core levels of bulk Ag crystals,[35] which was also observed in the XRD spectra (Fig. S3). Moreover, the narrow width of the peaks suggested that only a single element-silver was present in the system, and provided evidence for the encapsulation of zero valence AgNPs by HBMs templates. The binding energies at 284.82 eV, 399.36 eV and 530.92 eV were arisen from C1s, N1s and O1s respectively. The occurrence of carbon, nitrogen and oxygen signals confirmed the presence of HBMs on the surface of the AgNPs. The results of XPS spectra provided sufficient supporting evidence that HBMs were anchored on the surface of AgNPs and kept AgNPs against aggregation, and this was very crucial to obtain the highly stable conductive ink.

In order to validate the applicability of this fabrication strategy, the obtained AgNPs were redispersed into the mixture of ethylene glycol, ethanol and water to fabricate the AgNPs conductive ink

Cite this: DOI: 10.1039/c0xx00000x

www.rsc.org/xxxxxx

ARTICLE TYPE

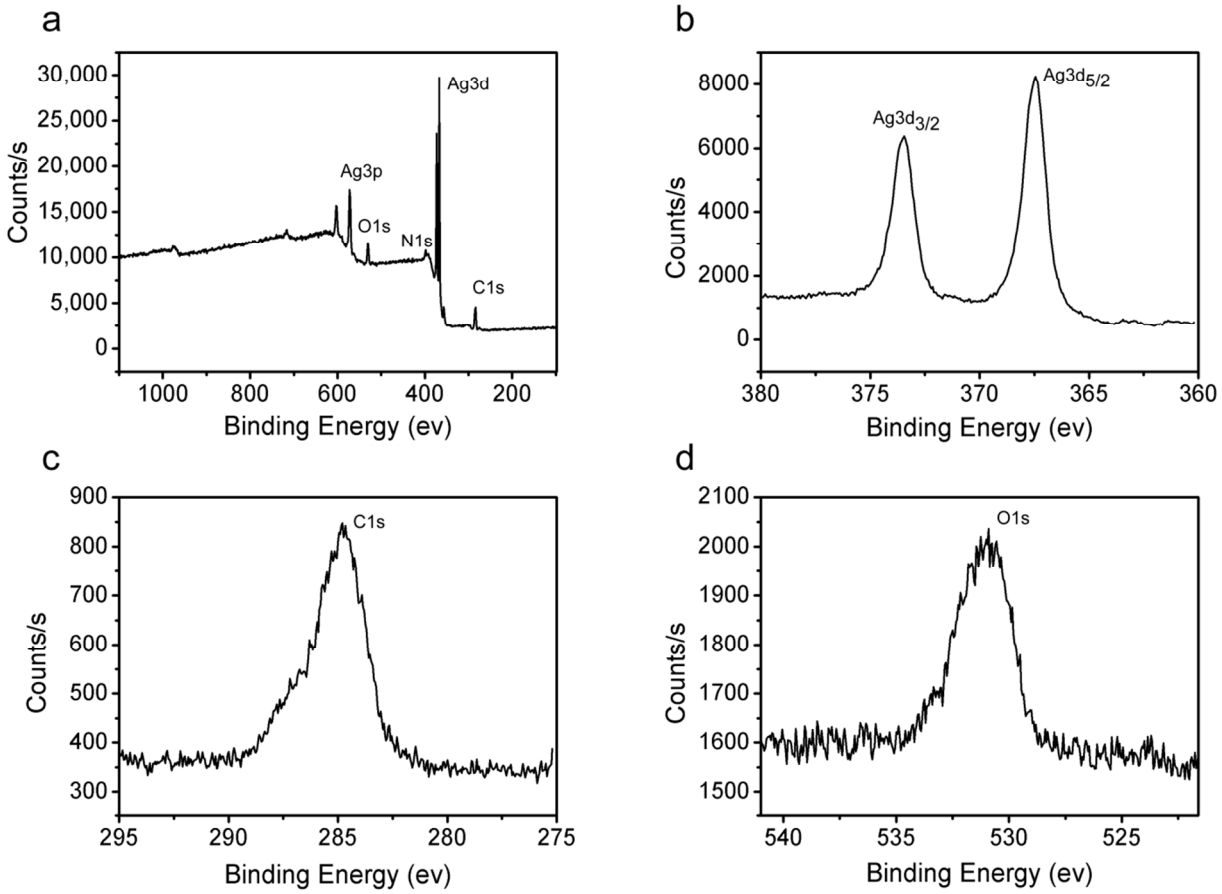

Fig. 3 XPS spectra of HBMs-encapsulated AgNPs: (a) XPS survey spectrum; (b) binding energy spectrum for Ag3d; (c) binding energy spectrum for of C1s and (d) binding energy spectrum for O1s.

for ink-jet printing flexible electrocircuits (Fig.4a). Compare to the other commercial AgNPs ink, the conductive ink based on as-synthesized AgNPs exhibited high stability due to the highly density functional groups on the HBMs periphery. These terminal groups could be anchored on the surfaces of AgNPs and effectively prevent the further agglomeration. As a result, the plasmon absorption band of the formed AgNPs ink exhibited no obvious change after storage for three months under ambient conditions (Fig.S4), revealing the high stability of the AgNPs ink fabricated by our strategy. More importantly, due to the nearly uniform shape and narrow size distribution, the conductive ink based on these synthesized nanoparticles demonstrated excellent printing fluency, and the printer nozzle would not be clogged with the larger nanoparticles or aggregation, which was very advantageous for ink-jet printing technique to fabricate flexible electrocircuits.[17]

According to the designs, a series of electrocircuits were fabricated by ink-jet printing the AgNPs ink onto PET film (Fig.4b). It showed that the straight and smooth conductive lines were obtained after solvent evaporation, and the coffee-ring effect was effectively depressed in a great degree. Morphological feature of the printed lines was evaluated by two dimensional analysis, and the topography of the printed electrocircuits remained flat with a relatively uniform thickness of 100 nm from the cross-sectional profile (Fig.S5), which was very favourable to obtain high conductivity. The surface morphology of the printed electrocircuits was further examined by SEM. From Fig. 4c, there were abundant AgNPs in the printed areas, and these AgNPs were stacked very densely due to convective flow during evaporation of the solvents.[36] However, the residual HBMs molecules capped on the surface of the nanoparticles, would seriously prevent electrons transfer from one nanoparticle to another and result in the relatively high resistivity with about 3.52×10^{-4} Ω.m owing to the scarcity of effectively conducting percolation paths.[37]

To improve the electrical conductivity, the printed flexible electrocircuits were sintered by a semiconductor laser. In order to evaluate the role of the laser during the sintering process, the morphology of AgNPs after sintering were investigated in detail. From the SEM image (Fig. 4d), the protective layers on the

Cite this: DOI: 10.1039/c0xx00000x

www.rsc.org/xxxxxx

ARTICLE TYPE

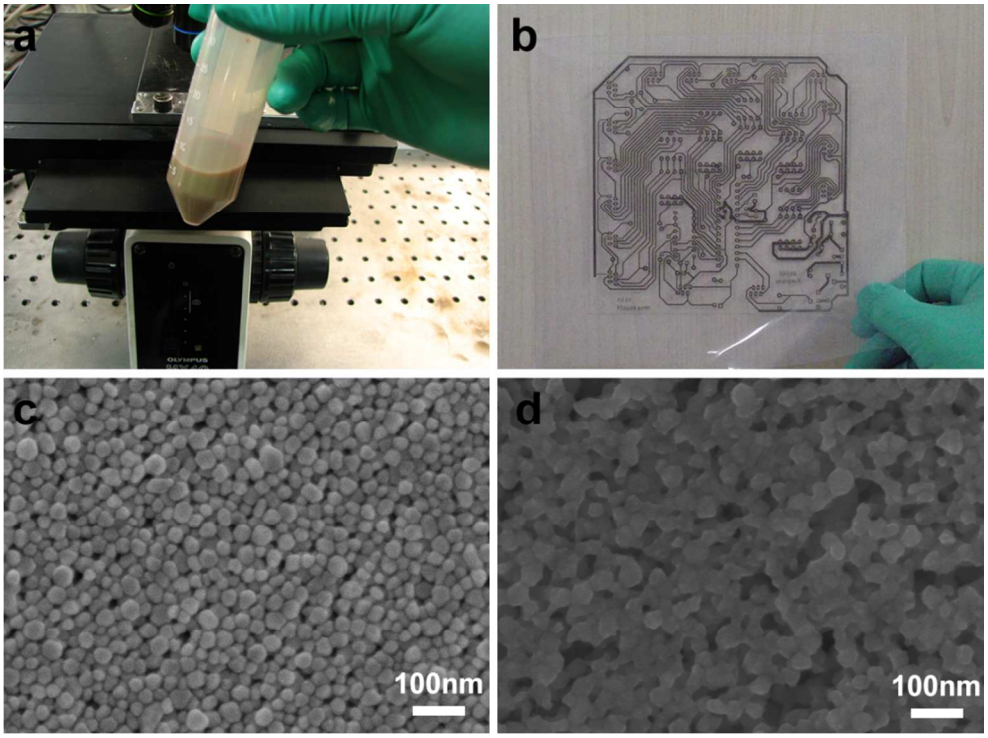

Fig.4 (a) Optical image of the formed AgNPs conductive ink; (b) the ink-jet printed flexible electrocircuits on PET substrate; (c) SEM image of the printed electrocircuits; (d) the surface topography changes after laser sintering treatment.

surfaces of AgNPs were effectively removed, and the surface morphology exhibited obvious changes due to the laser sintering treatment. The AgNPs changed from the uniform and spherical nanoparticles into bigger and irregular ones. It was noted that most AgNPs gradually contact, coalesce, and a lot of necks emerged among the AgNPs aggregate. Multiple percolation paths were continuously formed in the ink-jet printed electrocircuits, which was fairly pivotal to the electron transmission among AgNPs aggregate.[38] Consequently, the significantly lower resistivity value was achieved when the printed electrocircuits were sintered by a semiconductor laser (808 nm, 0.8 W), and the resistivity decreased in the range of 8.26×10^{-8}~7.62×10^{-8} Ω.m. Moreover, the resistance had no obvious change after storage for one month under ambient conditions, revealing the high stability of the ink-jet printed electrocircuits fabricated by our strategy. These performance could fully meet the demands of flexible electrocircuits in optoelectronic devices field, and promised enormous potential for manufacture of flexible electrocircuits, low cost electrodes and sensor devices.

Conclusions

In summary, a facile and efficient strategy was developed to controllable synthesis of AgNPs with different generation of HBMs as templates for ink-jet printed flexible electrocircuits. Nearly Uniform and monodisperse AgNPs in the range of 21.8±2.2 -31.2±3.6 nm have been successfully synthesized and redispersed to obtain highly stable condutive AgNPs ink. A series of flexible electrocircuits were fabricated by ink-jet printing the as-synthesized AgNPs on PET substrates, and exhibited low resistivity in the range of 8.26×10^{-8}~7.62×10^{-8} Ω.m after laser sintering treatment. This method successfully provided a facile approach to synthesize uniform and monodisperse nanomaterials and would have enormous potential in flexible electronic devices.

Acknowledgments

The authors would like to thank the National Nature Science Foundation (21303091, 21171019 and 21073203) and the Promotive Research Fundation for Excellent Young and Middle-aged Scientisits of Shandong Province (BS2013CL002).

Notes and references

[a] *Research Center of Analysis and Test, Qilu university of technology, Jinan 250353, China E-mail: zhzhl@iccas.ac.cn*

[b] *Beijing National Laboratory for Molecular Sciences (BNLMS), Institute of Chemistry, Chinese Academy of Sciences, Beijing 100190, China*

† Electronic Supplementary Information (ESI) available: [details of any supplementary information available should be included here]. See DOI: 10.1039/b000000x/

1. L. Yang, T. Zhang, H. Zhou, S. C. Price, B. J. Wiley and W. You, *ACS Appl Mater Interfaces*, 2011, 3, 4075-4084.
2. M.-C. Choi, Y. Kim and C.-S. Ha, *Prog Polym Sci*, 2008, 33, 581-630.
3. X.-Y. Zeng, Q.-K. Zhang, R.-M. Yu and C.-Z. Lu, *Adv Mater*, 2010, 22, 4484-4488.
4. W. Xu, J. Zhao, L. Qian, X. Han, L. Wu, W. Wu, M. Song, L. Zhou, W. Su, C. Wang, S. Nie and Z. Cui, *Nanoscale*, 2014, 6, 1589-1595.
5. B. Y. Ahn, E. B. Duoss, M. J. Motala, X. Guo, S.-I. Park, Y. Xiong, J. Yoon, R. G. Nuzzo, J. A. Rogers and J. A. Lewis, *Science*, 2009, 323, 1590-1593.
6. K. Higashitani, C. E. McNamee and M. Nakayama, *Langmuir*, 2011, 27, 2080-2083.
7. J. Lee, P. Lee, H. Lee, D. Lee, S. S. Lee and S. H. Ko, *Nanoscale*, 2012, 4, 6408-6414.
8. H.-Y. Ko, J. Park, H. Shin and J. Moon, *Chem Mater*, 2004, 16, 4212-4215.
9. B. S. Ong, Y. Li and Y. Wu, *J Am Chem Soc*, 2007, 129, 1862-1863.
10. S. Sivaramakrishnan, P. J. Chia, Y. C. Yeo, L. L. Chua and P. K. H. Ho, *Nature Materials*, 2007, 6, 149-155.
11. J. Eastoe, M. J. Hollamby and L. Hudson, *Adv Colloid Interfac*, 2006, 128-130, 5-15.
12. C.-D. Keum, N. Ishii, K. Michioka, P. Wulandari, K. Tamada, M. Furusawa and H. Fukushima, *J Nonlinear Opt Phys*, 2008, 17, 131-142.
13. M. Baghbanzadeh, L. Carbone, P. D. Cozzoli and C. O. Kappe, *Angew Chem Int Edit*, 2011, 50, 11312-11359.
14. N. A. Dhas, C. P. Raj and A. Gedanken, *Chem Mater*, 1998, 10, 1446-1452.
15. K.-S. Chou, Y.-C. Lu and H.-H. Lee, *Mater Chem Phys*, 2005, 94, 429-433.
16. M. Zhang, A. Zhao, H. Sun, H. Guo, D. Wang, D. Li, Z. Gan and W. Tao, *J Mater Chem*, 2011, 21, 18817-11824.
17. J. Park and J. Moon, *Langmuir*, 2006, 22, 3506-3513.
18. J. X. Dong, F. Qu, N. B. Li and H. Q. Luo, *RSC Advances*, 2015, 5, 6043-6050.
19. T. Yanagishita, Y. Maejima, K. Nishio and H. Masuda, *RSC Advances*, 2014, 4, 1538-1542.
20. H. Imai, Y. Takei, K. Shimizu, M. Matsuda and H. Hirashima, *J Mater Chem*, 1999, 9, 2971-2972.
21. W. Kwon and S.-W. Rhee, *Chem Commun*, 2012, 48, 5256-5258.
22. L. Jin, S.-P. Yang, H.-X. Wu, W.-W. Huang and Q.-W. Tian, *J Appl Polym Sci*, 2008, 108, 4023-4028.
23. R. Hourani, M. A. Whitehead and A. Kakkar, *Macromolecules*, 2008, 41, 508-510.
24. G. Franc and A. Kakkar, *Chem Commun*, 2008, 5267-5276.
25. M. Gladitz, S. Reinemann and H.-J. Radusch, *Macromol Mater Eng*, 2009, 294, 178-189.
26. M. Zhao, L. Sun and R. M. Crooks, *J Am Chem Soc*, 1998, 120, 4877-4878.
27. M. Stofik, Z. Stýhal and J. Malý, *Biosens Bioelectron*, 2009, 24, 1918-1923.
28. C.-Q. Shou, C.-L. Zhou, C.-B. Zhao, Z.-L. Zhang, G.-B. Li and L.-R. Chen, *Talanta*, 2004, 63, 887-891.
29. Z. Zhang, X. Zhang, Z. Xin, M. Deng, Y. Wen and Y. Song, *Adv Mater*, 2013, 25, 6714-6718.
30. Z. Zhang and W. Zhu, *J Mater Chem C*, 2014, 2, 9587-9591.
31. G. Mie, *Ann Phys-berlin*, 1908, 330, 377-445.
32. D. S. Wang and M. Kerker, *Appl. Opt.*, 1980, 19, 2135.
33. H. Wang, X. Qiao, J. Chen, X. Wang and S. Ding, *Mater Chem Phys*, 2005, 94, 449-453.
34. N. Zheng, J. Fan and G. D. Stucky, *J Am Chem Soc*, 2006, 128, 6550-6551.
35. J. Sharma, N. K. Chaki, A. B. Mandale, R. Pasricha and K. Vijayamohanan, *J Colloid Interf Sci*, 2004, 272, 145-152.
36. H. Hu and R. G. Larson, *Langmuir*, 2005, 21, 3963-3971.
37. J. Perelaer, M. Klokkenburg, C. E. Hendriks and U. S. Schubert, *Adv Mater*, 2009, 21, 4830-4834.
38. M. Layani, M. Gruchko, O. Milo, I. Balberg, D. Azulay and S. Magdassi, *ACS Nano*, 2009, 3, 3537-3542.